Food Control 171 (2025) 111086

Contents lists available at ScienceDirect

Food Control

journal homepage: www.elsevier.com/locate/foodcont

Recovery mechanisms of ohmic heating-induced sublethally injured *Staphylococcus aureus:* Changes in cellular structure and applications in pasteurized milk

Han Wang [a], Lele Shao [b], Yingying Sun [a], Yana Liu [a], Bo Zou [a], Yijie Zhao [a], Yuhan Wang [a], Xingmin Li [a], Ruitong Dai [a,*]

[a] College of Food Science and Nutritional Engineering, China Agricultural University, No.17 Qinghua East Road, Haidian District, Beijing, 100083, PR China
[b] College of Tea & Food Science and Technology, Anhui Agricultural University, No. 130 Changjiang West Road, Hefei, 230036, PR China

ARTICLE INFO

Keywords:
Sublethally injury
Ohmic heating
Staphylococcus aureus
Cellular structure
Recovery
Bacteriostatic agents
Pasteurized milk

ABSTRACT

This study investigated the alterations in cellular structure of ohmic heating (OH)-induced injured *Staphylococcus aureus* (*S. aureus*) during repair in nutrient broth, and the potential antibacterial approach of combining OH with food bacteriostatic agents and their application in milk. Specifically, the biological properties (surface hydrophobicity, zeta potential, particle size) and indicators related to cell membrane and cell wall integrity (peptidoglycan content, activities of β-galactosidase, alkaline phosphatase, and lactate dehydrogenase) of injured *S. aureus* during repair were measured. Additionally, scanning electron microscope and transmission electron microscope analyses were used to observe morphological changes, and protein changes were analyzed using fourier transform infrared spectroscopy and sodium dodecyl sulfate-polyacrylamide gel electrophoresis. The results suggested that OH destroyed the biological properties and membrane structure (membrane integrity and permeability increased, cell wall integrity increased, protein and functional group of membrane were damaged) of *S. aureus*, which could be partially restored after repair. However, the restoration process between cell membrane and cell wall were inconsistent, and morphological changes reinforce these findings. Notably, membrane proteins and functional groups on the bacterial cell surface were difficult to repair. Also, OH combined with low doses of bacteriostatic agents is a potential method to ensure food safety. Carvacrol and low temperatures could inhibit the repair of injured bacteria in pasteurized milk; and reduce precipitate formation and putrid gas production.

1. Introduction

Foodborne illnesses are a significant public health concern worldwide, commonly arising from the ingestion of toxic or pathogenic microorganisms. According to the World Health Organization (WHO), around 420,000 people die each year from eating contaminated food (WHO, 2024). *Staphylococcus aureus* (*S. aureus*), a widespread foodborne pathogen that causes approximately 20%–25% of bacterial foodborne disease outbreaks and can be found in milk and dairy product, raw meat, as well as aquatic products (Li et al., 2022; Zhen et al., 2024). When these products become contaminated, *S. aureus* is capable of secreting various enzymes (*e.g.,* hemolysin) and toxins (*e.g.,* enterotoxin) that pose a risk to human health (Shao, Zhao, Zou, Li, & Dai, 2022), and these virulence factors can cause infections to escalate into severe, life-threatening conditions such as necrotizing fasciitis, endocarditis, and pneumonia (Kobayashi, Malachowa, & DeLeo, 2015; Tong Steven, Davis Joshua, Eichenberger, Holland Thomas, & Fowler Vance, 2015). As a result of *S. aureus* contamination, foodborne illnesses and outbreaks can occur, leading to significant human casualties and substantial economic losses worldwide (Li et al., 2022). For example, between 2010 and 2020, over 700 cases of *S. aureus*-related food safety incidents were reported in China (LIU Tingting et al., 2022), while similar outbreaks have been documented in other countries, including Canada, the United States, Australia, *etc* (Ikuta et al., 2022). Therefore, controlling the growth and reproduction of *S. aureus* is critical for preventing foodborne illnesses and safeguarding public health on a global scale.

Ohmic heating (OH) represents an innovative processing technology that addresses some of the limitations of conventional heat treatments,

* Corresponding author. College of Food Science & Nutritional Engineering, China Agricultural University, P.O. Box 303, Beijing, 100083, PR China.
E-mail address: dairuitong@hotmail.com (R. Dai).

https://doi.org/10.1016/j.foodcont.2024.111086
Received 21 August 2024; Received in revised form 1 December 2024; Accepted 3 December 2024
Available online 5 December 2024
0956-7135/© 2024 Elsevier Ltd. All rights are reserved, including those for text and data mining, AI training, and similar technologies.

such as energy inefficiency and negative impacts on food quality and is widely applied in the food industry (Shao et al., 2023; Sakr, & Liu, 2014). Unlike conventional heating methods, the OH transforms electrical energy directly into thermal energy by using the food material as a resistor, providing faster and more uniform heating (Gavahian, 2018). This rapid, uniform heating results in efficient enzyme and microbial inactivation, making OH a highly effective alternative to traditional thermal processing methods and attracting significant attention from researchers in recent years for its potential to improve food safety and processing efficiency (Makroo, Rastogi, & Srivastava, 2020). However, research has shown that bacteria may enter a sublethally injured state during OH treatment due to environmental stresses, characterized by their inability to grow on selective media as a result of cell membrane damage and the leakage of intracellular macromolecules (Shao et al., 2020; Tian, Yu, Shao, Li, & Dai, 2018; Zhang, Lan, & Shi, 2021b). To the best of our knowledge, most current studies on the repair of sublethally injured cells have concentrated on optimizing repair conditions, such as nutrient richness, temperature, pH, and the role of metal ions in the repair process. Few studies, however, have explored repair mechanisms from the perspective of cellular structure (Lan, Zhang, Zhang, & Shi, 2019; Lan et al., 2022; Shao et al., 2022).

Essential oils (EOs) and polyphenol monomers (PMs) are secondary metabolites of plants, typically extracted from various plant parts such as leaves, seeds, and roots (Huang, Liu, Jia, Zhang, & Luo, 2017). In the field of food safety and microbiology, common EOs include tea tree oil, lemon essential oil, and carvacrol (Pedreira, Martínez-López, Vázquez, & García, 2023; Wei et al., 2023; Yazgan, Ozogul, & Kuley, 2019), while typical PMs include gallic acid, chlorogenic acid, and rutin (Al-Shabib et al., 2017; Qu et al., 2023; Santana-Gálvez, Cisneros-Zevallos, & Jacobo-Velázquez, 2017). These substances, due to their antimicrobial and antioxidant properties, have been explored as natural alternatives to synthetic food additives (Tongnuanchan, 2014). In this study, we refer to these substances as bacteriostatic agents. Furthermore, the potential synergistic effects of novel technologies, in combination with EOs and PMs, have also been investigated for enhancing bactericidal activity (de Souza Pedrosa et al., 2021). However, the effectiveness of combining OH with bacteriostatic agents in inhibiting damaged bacteria remains unclear. This study also explores the application of this combined treatment method in pasteurized milk, a product susceptible to bacterial contamination post-processing. Improper packaging or storage may allow for the growth of residual or newly introduced bacteria, posing a risk to consumer health (Ortuzar et al., 2018). Ultimately, this research aims to provide theoretical support for the development of new combined treatment strategies to improve food safety.

The aim of this study is to investigate the changes in cell wall and cell membrane integrity during the repair process and assess the effects of chlorogenic acid, gallic acid, tea tree oil, and carvacrol on the recovery of injured S. aureus cells. The study is guided by three research questions (RQs) as follows; RQ1: What are the alterations in the membrane structure of sublethally injured *S. aureus* cells after OH treatment and during the repair process? This question explores the changes in membrane integrity by examining variations in biological properties, cell membranes, cell walls, and associated proteins and enzymes during the repair of sublethally injured *S. aureus* cells. RQ2: Is it feasible to ensure food safety by combining mild OH processing with low doses of bacteriostatic agents? To address this, the study investigates whether a combination of mild OH treatment and low doses of bacteriostatic agents can effectively inhibit bacterial recovery, employing four different bacteriostatic agents at varying concentrations. RQ3: What are the effects of carvacrol and temperature on the growth of sublethally injured *S. aureus* in pasteurized milk, and how do these factors influence the visual changes in the milk? By controlling carvacrol concentration and storage temperature, this research assesses the growth of sublethally injured *S. aureus* in pasteurized milk and monitors any visual changes in the milk.

2. Materials and methods

2.1. Bacterial strain and culture condition

The bacterial cultivation process is based on the research published by Shao et al. (2020). *S. aureus* strain ATCC 6538 (Shanghai Huiyun Biological Co., Ltd., China) was stored at - 80 °C with 30% glycerol. The cells were then sub-cultured by placing them onto a nutrient agar (NA) medium from Beijing Solarbio Co., Ltd., China, and incubated at 37 °C for 24 h to allow colony formation. After incubation, a single colony was taken and inoculated into 20 mL of nutrient broth (NB) from Beijing Solarbio Co., Ltd., China in a shaker, set to 37 °C and 180 rpm, for 12 h. Subsequently, small volume (200 μL) of this initial culture was transferred to a larger volume (200 mL) of NB and incubated at 37 °C until the culture reached the mid-logarithmic growth phase (approximately 3.5 h). The *S. aureus* pellets were collected by centrifugation at 8000×*g*, at 4 °C, for 10 min using a TGL-20M centrifuge from Pingfan Instrument, China. The centrifuged pellets were then washed twice with phosphate buffer solution (PBS), pH 7.2 ± 0.1. The microspheres were then resuspended in PBS to create a bacterial suspension with an approximate concentration of 2×10^8 colony-forming units per milliliter (CFU/mL).

2.2. Ohmic heating treatment

The OH treatment processing was conducted according to our published work (Wang et al., 2024). The bacterial suspension in PBS was pre-adjusted to 25 °C before treatment. Thereafter, a 160 mL volume of the bacterial suspension was added to the heater and a voltage gradient of 10 V/cm and a frequency of 50 Hz were applied during the heating. The suspension was heated for a total duration of 100 s, after which it was immediately placed at 4 °C to halt further heating. Based on our preliminary experimental results, NA supplemented with 10% NaCl was used as the selective medium to identify sublethally injured cells. The experimental setup showed that at a temperature of 55.5 °C, the injury rate of the cells exceeded 95%, meeting the criteria needed for further experiments. For the recovery treatment, the injured *S. aureus* cells were incubated in NB at 37 °C with shaking at 180 rpm for 3 h. This treatment allowed for complete repair of the sublethally injured cells. The sublethally injured ratio was determined using the following equation (Wang et al., 2024):

$$\textit{The injury ratio}\ (\%) = 100 - \frac{CFU \mid mL_{NA-NaCl}}{CFU \mid mL_{NA}} \times 100 \quad (1)$$

2.3. Surface hydrophobicity, zeta position, and size measurements

Bacterial suspensions from the mid-exponential growth phase, OH-induced injured state, and various periods of the repaired state were washed twice and then resuspended in equal volume of PBS. Surface hydrophobicity was analyzed as described previously (Lv et al., 2019). The optical density $(OD)_{600}$ values of each bacterial suspension were recorded and labeled as A_0, representing the initial absorbance of each suspension. To test hydrophobicity, 0.5 mL of hexadecane was added to 3 mL of the bacterial suspension, vortexed for 2 min to allow interaction between the bacterial cells and hexadecane, and then left at room temperature for 15 min to allow the phases to separate. The supernatant was then slowly collected by pipette, and the OD_{600} value was recorded as A_1. Surface hydrophobicity was calculated using the following equation (Lv et al., 2019; Noma et al., 2017):

$$\text{surface hydrophobicity}\ (\%) = \frac{A_0 - A_1}{A_0} \times 100\ (\%) \quad (2)$$

The Malvern electrochemical workstation was used to measure zeta potential and particle size. The bacteria samples were washed twice with PBS to remove any residual media or buffer and then resuspended in distilled water to prepare them for measurement. Before measurements,

the workstation was preheated for 30 min, and the measurement vessel was thoroughly cleaned by washing it at least three times with distilled water to ensure accuracy and avoid contamination.

2.4. Membrane potential and integrity

Membrane potential was assessed using a cell membrane potential assay kit (JC-1, fluorescence probe detection method, detected by fluorescence spectrum detector) (C2006, Beyotime Biotech. Inc.) following the method described by Wang et al. (2023). The concentrations of untreated, OH-treated, and repaired *S. aureus* cells were adjusted to appropriately 1×10^6 CFU/mL. Half a milliliter of the bacterial solution was mixed with JC-1 staining solution and then incubated in the dark at 37 °C for 20 min. The mixture was subsequently centrifuged (600×*g*, 4 °C, 5 min), washed twice with a specialized buffer, and resuspended for fluorescence intensity detection at emission (green fluorescence) and excitation (red fluorescence) wavelengths of 590 nm and 525 nm, respectively. The membrane potential value was expressed as the ratio of emission to excitation fluorescence intensity. For the assessment of membrane integrity, a modified method based on Shao et al. (Shao et al., 2023) was employed. PI stock solution (C0080, Solarbio Co., LTD., China) was added to 1 mL of bacterial suspension to achieve a final PI concentration of 5 μM. Fluorescence spectrum detector were used to determine fluorescence with excitation and emission wavelengths of 535 nm and 615 nm, respectively.

The activity of lactate dehydrogenase (LDH) was assessed using microplate method according to the kit introduction provided by Nanjing Jiancheng Biotechnology Co., LTD (Bai et al., 2023). After collecting the cells, an extraction solution was added to the samples, which were then subjected to ultrasound in an ice bath at a power setting of 200–300 W, with ultrasound applied for 5 s, followed by a 10 s pause, repeated for a total of 20 cycles. Then, centrifuge to obtain supernatant, which was prepared and mixed with buffer, a coenzyme, and 2,4-dinitrophenylhydrazine sequentially. After incubating at 37 °C for 15 min, sodium hydroxide was added, and the mixture was incubated again before adding the developer. The absorbance at a wavelength of 440 nm was recorded.

2.5. Cell wall integrity

Alkaline phosphatase (AKP) is a protease located between the cell wall and cell membrane, and is commonly used to assess cell wall integrity (Wang et al., 2017). The enzyme activity for AKP was determined following instructions from assay kits provided by Nanjing Jiancheng Biotechnology Co., Ltd., using the microplate method by microplate reader (Bai et al., 2023). After collecting the cells, an extraction solution was added to the samples, which were then subjected to ultrasound in an ice bath at a power setting of 200–300 W, with ultrasound applied for 5 s, followed by a 10 s pause, repeated for a total of 20 cycles. Then, the supernatant was mixed with buffer and substrate and incubated at 37 °C for 15 min. After the developer was added, the value was recorded at a wavelength of 520 nm.

Cell wall integrity was assessed by measuring β-galactosidase activity and peptidoglycan content (Ning et al., 2022; Shu et al., 2022). The activity of β-galactosidase was measured using an assay kit (BC2580, Solarbio Co., Ltd., China) following the kit instructions. Untreated, OH-treated, and repaired *S. aureus* cells were prepared by centrifugation at 8000×*g* at 4 °C for 10 min, washed twice with PBS to remove any residual substances, after which the supernatant was discarded. A specialized extraction solution was added to the cells, which were then disrupted by ultrasonic crushing in an ice bath set to 200 W, applying 3 s pulses with 10 s pauses in between, for a total duration of 10 min. The disrupted samples were then centrifuged at 15,000×*g* at 4 °C for 10 min, and the supernatant was collected and kept on ice for measurement. The spectrophotometer was preheated for 30 min before detection at 400 nm. The peptidoglycan content was determined by Purified PG antibody method, using a microbial peptidoglycan ELISA assay kit (Jiangsu Meimian Industrial Co., Ltd). Bacterial cells in different states were disrupted using ultrasonic crushing in an ice bath at 300 W, with 3 s pulses and a 10 s pause, for a total of 10 min. The disrupted samples were then centrifuged to obtain the supernatant for analysis. The absorbance at a wavelength of 450 nm was recorded within 15 min after the reaction was terminated.

2.6. Cell morphology

Scanning electron microscopy (SEM) and transmission electron microscopy (TEM) are powerful tools used to observe morphology changes in *S. aureus* cells during sublethal injury and recovery in NB. The preparation protocol followed the method described by Zhao, Shao, Jia, Zou, et al. (2022), which is summarized as follows: bacterial suspensions from the mid-exponential growth, OH-induced injury, and various stages of repair were washed twice with PBS and centrifuged at 4 °C, 8000×*g* for 10 min to obtain the pellet in centrifuge tubes. Subsequently, 3% of pentanediol was added to the centrifuge tubes, and the samples were immersed at 4 °C for 24 h. Afterward, bacteria were washed three times with PBS, and 1% osmium acid was used for bacterial encapsulation for 4–6 h. The samples were then washed three times with PBS and dehydrated in an ethanol gradient (10%, 30%, 50%, 70%, 90%, and 100%) for 10 min at each concentration.

For SEM analysis, samples were rinsed twice with isoamyl acetate (purity 100%) for 15 min each, after which the pellet were sprayed on a copper grid, dried at the critical point, and gold-coated. For TEM analysis, pretreated samples were immersed in a mixture of acetone and epoxy resin for 24 h, then polymerized at 60 °C for 48 h, sectioned into 50-nm slices, placed on a copper grid, and then observed and imaged using TEM.

2.7. Fourier Transform Infrared Spectrometer spectra analysis

The infrared spectra of intact, OH-treated, and recovered *S. aureus* cells were analyzed using a Fourier Transform Infrared Spectrometer (FTIR) spectrometer (Nicolet iS10 FT-IR spectrometer, USA) following the method described by Zhao, Shao, Jia, Zou, et al. (2022). Bacterial pellets were prepared according to the method outlined in section 2.6, then vacuum freeze-dried for 48 h to obtain the bacteria in powdered form. Two milligrams of each sample were mixed with 100 mg dry KBr, uniformly ground, and compressed into tablets at 20 MPa pressure. The prepared samples were scanned on the FTIR spectrometer with the resolution of 4 cm^{-1} over a range of absorption peak from 4000 to 400 cm^{-1}. The resulting spectra were analyzed using Origin 2021 and Peakfit V 4.12 software.

2.8. Whole cell proteins and membrane proteins analysis

The analysis methods of whole cell proteins and membrane proteins were based on previous research (Huang, Jia, Zhang, Liu, & Luo, 2019; Wang et al., 2020). Bacterial pellets were obtained following the method described in section 2.6. Lysis buffer and enzyme inhibitor (R0010, Solarbio Co., Ltd., China) were added to the pellets and thoroughly mixed. The suspension was then incubated at 4 °C for 30 min with intermittent shaking every 10 min for 5 s. Subsequently, the samples were subjected to ultrasonic disruption (ice-bath, 200 W, 3 s impulse, 10 s pause, 10 min), and centrifuged at 10, 000×*g* for 3 min at 4 °C to obtained the supernatant. The protein concentration in the supernatant was determined using a BCA kit (PC0020, Solarbio Co., Ltd., China), and the protein concentration of each group was adjusted to ensure consistency. For SDS-PAGE analysis, 10 μL of supernatant was mixed with 40 μL of 5 × loading buffer, boiled for 10 min, and then centrifuged at 10, 000×*g* for 5 min. Subsequently, 20 μL of the supernatant was loaded onto the gel, electrophoresis apparatus was used in the next step. Cell membrane proteins of *S. aureus* were extracted following the

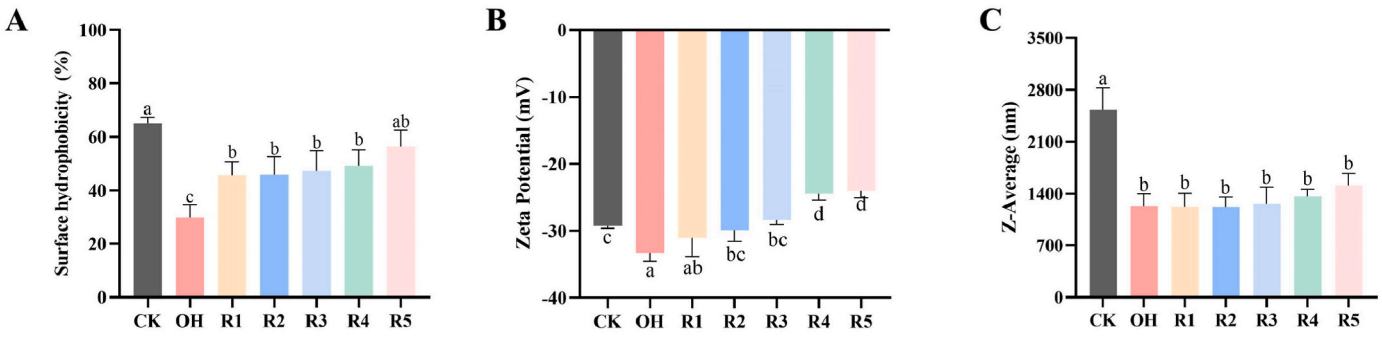

Fig. 1. Biological properties of OH-induced sublethally injured *S. aureus* cells during repair. (A) Surface hydrophobicity, (B)zeta potential, and (C) particle size of *S. aureus* cells. CK: untreated cells; OH: ohmic heating treated cells; R1 to R5: recovered in nutrient broth for 1–5 h. Values were means ± standard deviation of three replicates. Capital letters a ~ c represent the significant difference under different recovery time ($p < 0.05$).

instructions of the extraction kit (BB-3151, BestBio, Co., Ltd., China). All tools used in the membrane protein extraction process were pre-cooled at −20 °C, and samples were maintained at a low temperature throughout the extraction process. After adjusting the protein concentrations of each group to ensure consistency, they were mixed with the 5 × loading buffer, incubated at 50 °C for 30 min, centrifuged, and 20 μL of the supernatant were used for SDS-PAGE analysis, and SDS-PAGE images were displayed via Gel imager.

2.9. The inhibition of repair by bacteriostatic agents

Chlorogenic acid (C109402) was purchased from Aladdin Chemistry (Shanghai, China), gallic acid (G823163), tea tree oil (T819562), and carvacrol (C804847) were purchased from McLean Biochemical Technology (Shanghai, China). Chlorogenic acid and gallic acid are PMs, and tea tree oil and carvacrol are EOs. Stock solutions of bacteriostatic agents were prepared following a previously reported method (Zhang, Lan, & Shi, 2021a). The agents were dissolved in 40% ethanol to achieve a final concentration of 10 mg/mL and placed at 4 °C in the dark. The stock solutions were then serially double diluted with NB containing injured *S. aureus* cells. The final concentration of *S. aureus* cells was adjusted to 10^6 CFU/mL and the concentrations of inhibitor ranged from 0.039 to 10 mg/mL in successive dilutions. Minimum inhibitory concentration (MIC) of different bacteriostatic agents were determined after incubated at 37 °C for 16 h. In this experiment, the ethanol concentration used did not affect the growth of *S. aureus* (data not shown), and NB without the addition of bacteriostatic substances served as a control. In addition, four progressively decreasing concentrations of each bacteriostat were used to inhibit the repair of damaged bacteria in NB. For tea tree oil and the two PMs (chlorogenic acid and gallic acid), the four final concentrations selected in this experiment were 0.625 mg/mL, 0.313 mg/mL, 0.156 mg/mL, 0.078 mg/mL, respectively. The four final concentrations selected for carvacrol were 0.078 mg/mL, 0.039 mg/mL, 0.020 mg/mL, 0.010 mg/mL, respectively. Sublethally injured *S. aureus*

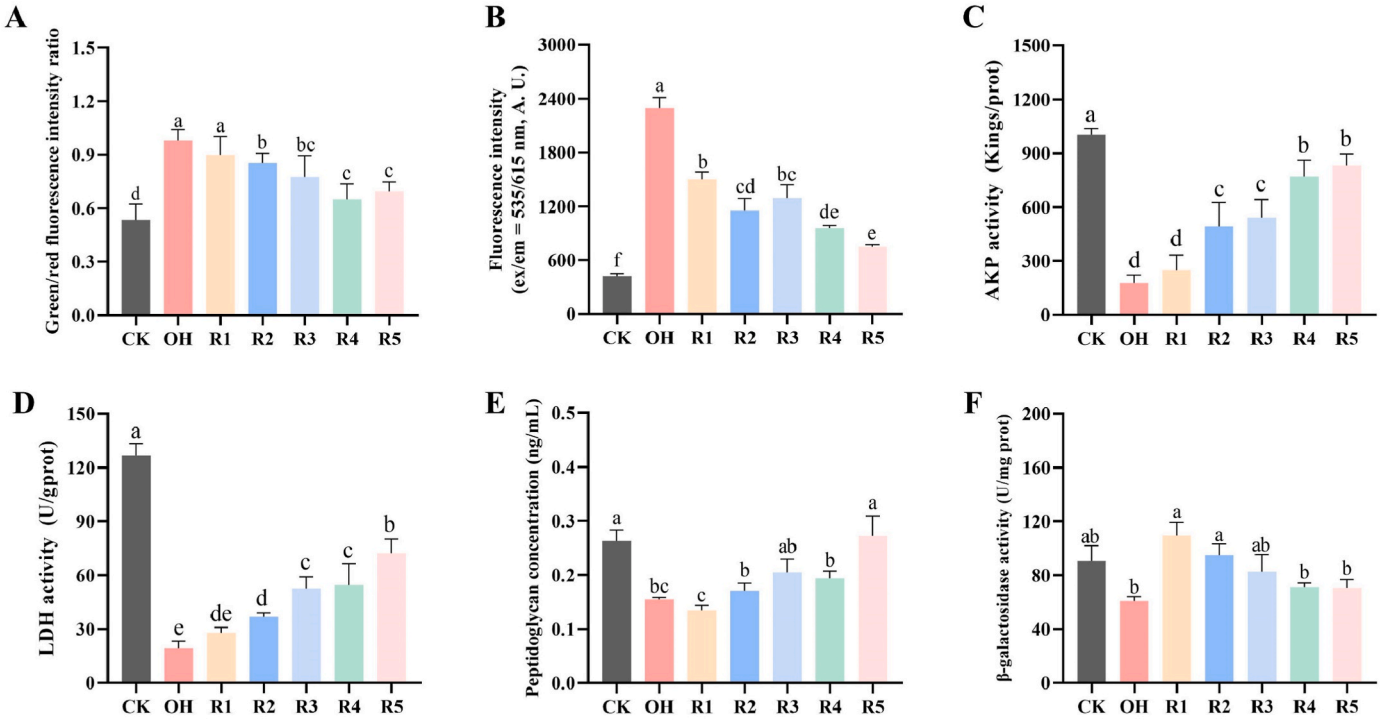

Fig. 2. Effects of different repair duration on cell membrane intergaty (A), permeability (B), AKP activity (C), LDH activity (D), peptidoglycan concentration (E) and β-galactisudase activity (F). CK: untreated cells; OH: ohmic heating treated cells; R1 to R5: recovered in nutrient broth for 1–5 h; AKP: alkaline phosphatase; LDH: lactic dehydrogenase. Values were means ± standard deviation of three replicates. Capital letters a ~ e represent the significant difference under different recovery time ($p < 0.05$).

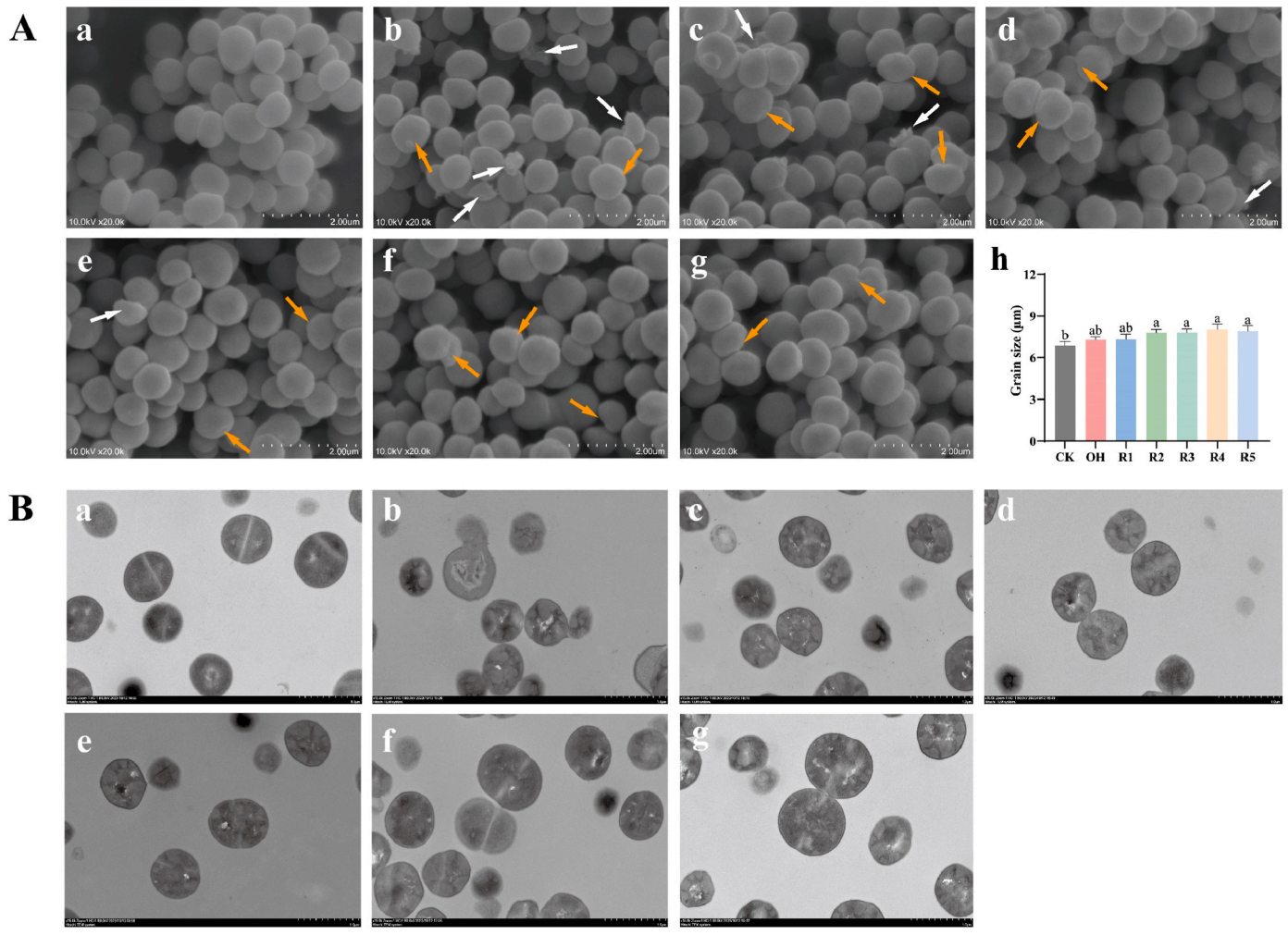

Fig. 3. SEM and TEM images of OH-induced sublethally injured *S. aureus* cells during recovery. (A, ã g) represent the control group, OH treatment group, repair for 1–5 h group, respectively. (A-h) Diameter of *S. aureus* cells. (B) TEM images of OH-induced sublethally injured *S. aureus* cells during recovery. (B- a ~ g) represent the control group, OH treatment group, repair for 1–5 h group, respectively. CK: untreated cells; OH: ohmic heating treated cells; R1 to R5: recovered in nutrient broth for 1–5 h; Values were means ± standard deviation of three replicates. Capital letters a ~ e represent the significant difference under different recovered time ($p < 0.05$). Orange arrow: cell deformation; white arrow: cell debris. (For interpretation of the references to colour in this figure legend, the reader is referred to the Web version of this article.)

cells were collected and resuspended in NB containing antibacterial agents, followed by incubation at 37 °C for 3 h. Plate count analysis was performed at 1 h intervals, using NB without bacteriostatic agents as the control culture medium.

2.10. Effects of carvacrol on the growth of sublethally injured S. aureus in pasteurized milk

Bacterial pellets were obtained following the method described in section 2.6. Bacteria were resuspended in equal volumes of pasteurized milk, followed by the adding of different concentration of carvacrol. The pasteurized milk was then divided into two groups and stored at 4 °C and 25 °C, respectively. The number of intact bacteria versus sublethally damaged bacteria was recorded at 0, 6, 12, 24, 48 and 72 h. Finally, 15 mL of treated pasteurized milk was poured into a glass culture dish and left to stand for 30 min, after which the supernatant was removed, and the precipitate was observed.

2.11. Statistical analysis

All experiments were conducted in triplicate, and data analysis was carried out using SPSS Statistics 26.0 software (IBM Corporation, Chicago, IL, USA). One-way analysis of variance (ANOVA) followed by Duncan's post-hoc tests were used to compare differences among all experiment groups. Statistical significance was set at $p < 0.05$. Graphical visualization of the results was performed using GraphPad Prism 8 (GraphPad Software Inc., San Diego, CA, USA).

3. Results

3.1. Changes in biological properties during repair

Changes in surface hydrophobicity and zeta potential of *S. aureus* in different states were measured to explore these biological properties. As shown in Fig. 1 A, compared to the control (CK) group, the surface hydrophobicity of *S. aureus* injured by OH treatment significantly decreased ($p < 0.05$). After 1 h of repair, the surface hydrophobicity of the *S. aureus* cells increased significantly compared to their unrepaired states, returning to levels similar to the untreated group after 5 h. The presence of charged amino acids in membrane proteins and anionic components, such as carboxyl and amino groups in the cell wall, contribute to the negative zeta potential of *S. aureus*. In Fig. 1 B, compared to intact *S. aureus* cells, the absolute zeta potential values of injured cells significantly increased, indicating enhanced mutual

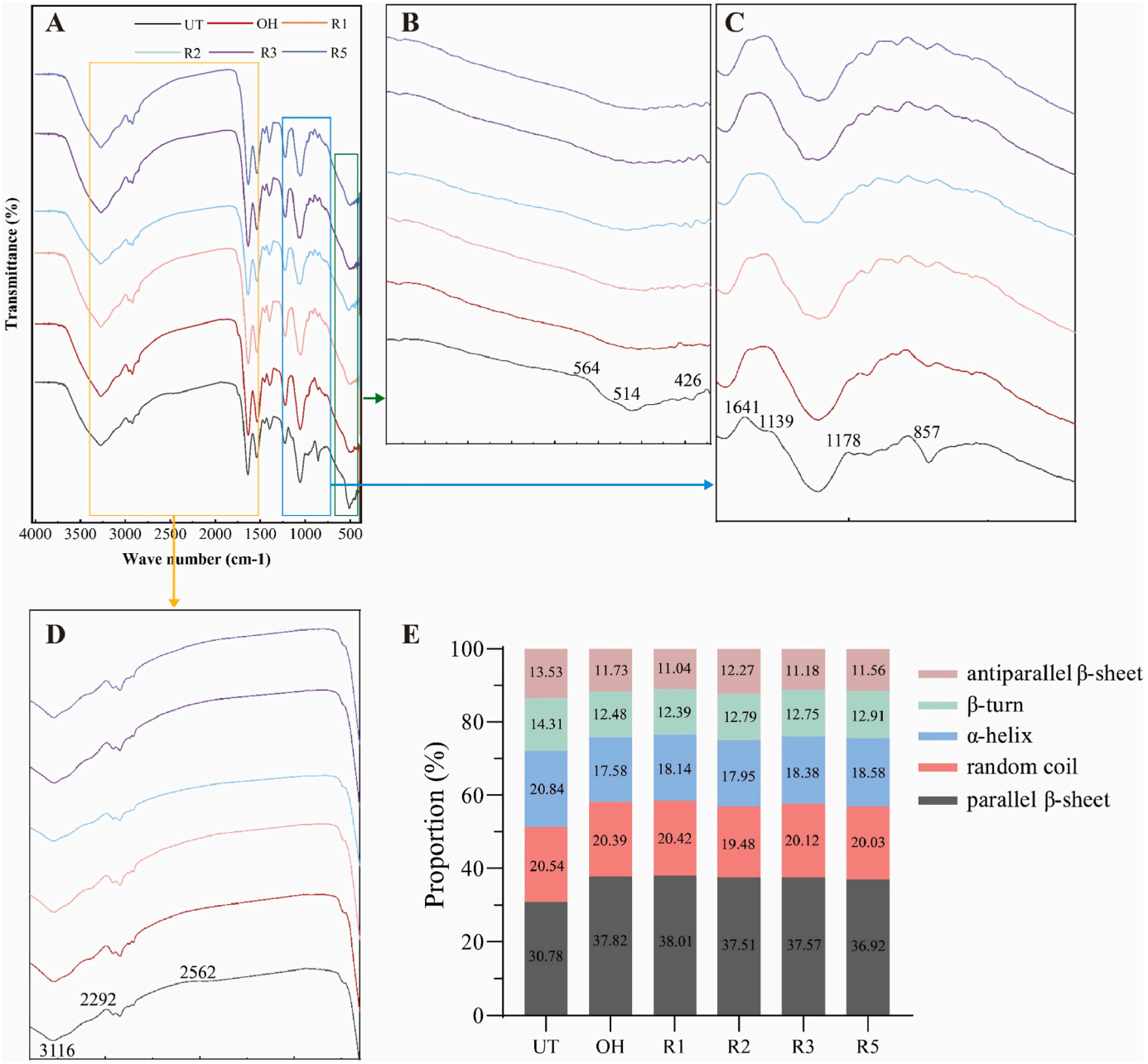

Fig. 4. (A) FTIR spectra of *S. aureus* cells before OH treatment and during repaired in NB; (E) Alternations in the secondary structure of cellular proteins. CK: untreated cells; OH: ohmic heating treated cells; R1 to R5: recovered in nutrient broth for 1–5 h.

repulsion between cells. Incubation in NB resulted in a gradual decrease in the absolute zeta potential value. After 2 h, a significant difference was observed between the cells incubated in NB for 2h and the unrepaired *S. aureus* cells, indicating reduced intercellular repulsion.

To further investigate whether OH treatment induced aggregation behavior in *S. aureus* cells, which could enhance resistance, particle size was examined. In Fig. 1 C, the particle size of injured cells was significantly smaller compared to untreated cells, suggesting a lack of aggregation behavior. Although particle size increased during the repair process, after 5 h of repair, there was no significant difference compared to unrepaired cells, and it remained notably lower than that of the untreated group.

3.2. Changes of cell membrane and cell wall during repair

This section examines indices related to the bacterial cell membrane. As depicted in Fig. 2 A, OH treatment significantly elevated the ratio of green to red fluorescence intensities compared to the CK group. Cell membrane integrity is assessed by the cells' capacity to uptake PI, which binds to DNA through damaged membranes, emitting red fluorescence. Nonetheless, OH treatment compromised the cell membrane integrity of *S. aureus*, leading to cell death and injury. During the repair process, both membrane potential and integrity gradually recovered, suggesting a reduction in membrane damage. Specifically, the green-red fluorescence intensity ratio significantly decreased after 2 h of repair, and membrane integrity was significantly improved after 1 h of repair compared to unrepaired *S. aureus* cells.

Besides, as depicted in Fig. 2C and D, levels of AKP and LDH decreased significantly in OH-induced sublethally injured cells compared to untreated cells ($p < 0.05$), and these two enzyme levels gradually upregulate during recover in NB and remained notably lower than that of the untreated group. As illustrated in Fig. 2E, peptidoglycan

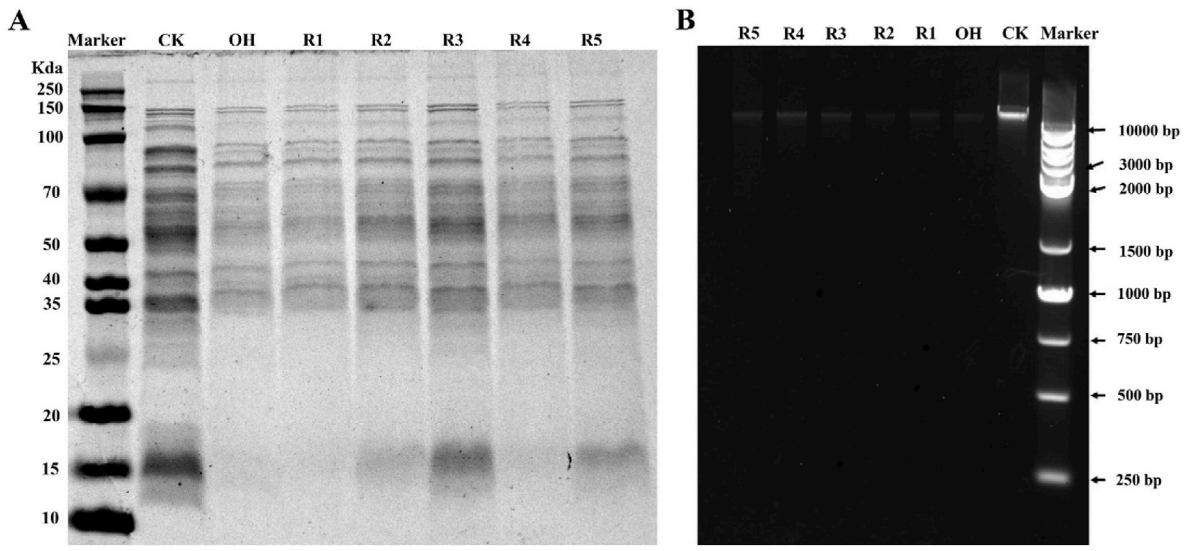

Fig. 5. A: SDS-PAGE pattern of cell membrane proteins of *S. aureus* treated with OH and repaired in NB. CK: untreated cells. B: agarose gel electrophoresis of *S. aureus* DNA treated with OH treatment and repaired in NB. CK: untreated cells; R0: ohmic heating treated cells without repair; R1 to R5: recovered in nutrient broth for 1–5 h.

content was markedly diminished in injured cells compared to intact cells from the CK group. During the repair process, peptidoglycan content increased during the repair process; after 5 h, it was significantly higher compared to unrepaired cells, returning to levels observed in untreated cells (Fig. 2E). Additionally, the activity of β-galactosidase was significantly decreased in injured *S. aureus* cells versus the intact cells from the CK group (Fig. 2F). During repair in NB, a sharp increase in galactosidase activity was triggered initially, followed by a gradual decrease.

3.3. Ultrastructure changes of sublethally injured cells during repair

SEM was utilized to investigate the morphological characteristics of sublethally injured *S. aureus* cells and their changes during repair, as shown in Fig. 3 B a-g. Untreated cells appeared round, with smooth, intact borders and a uniform size. However, after treatment with OH at 10 V/cm, 50 Hz for 100 s, surface wrinkles, irregular deformations, and fissures were observed, with some cells ruptured, and releasing cellular debris and contents. This indicates that OH treatment disrupts the outer membrane and alters cell morphology significantly. During repair in NB, the wrinkling and deformation of the bacterial surface gradually improved. After 3 h of repair, most cells appeared intact, although some cellular contents and debris were still observable. By 5 h, nearly all *S. aureus* cells had regained their complete borders. Noticeably, the cell diameter increased after OH treatment and remained larger than untreated cells after repair, possibly due to changes in the membrane structural composition.

Furthermore, TEM was utilized to analyze the changes in the internal structure of *S. aureus* during recovery (Fig. 3 A a-g). Untreated bacteria exhibited smooth cell surfaces, intact cell membranes and walls, and a uniform distribution of intracellular material. In contrast, OH-induced injured cells exhibited compromised structures, including incomplete cell membranes and walls, clumping of protoplasmic content, leakage, and vacuolation. This suggests that OH treatment destroys bacterial structures, leading to content leakage and cell injury or death. The trends observed in TEM during repair mirrored SEM observations, with injured cell structures gradually restoring. While most cells exhibited complete cellular structure after repair for 3 or 5 h, differences from untreated cells persisted. In summary, OH treatment disrupts the cellular structure of *S. aureus* cells, inducing a sublethal state, with the structural restoration of the injured cells occurring gradually during repair. These findings underscore the importance of measuring indicators of cellular structural integrity to effectively elucidate the repair mechanisms.

3.4. FTIR spectra analysis of S. aureus cells in different states during repair

FTIR analysis was conducted to gain deeper insight into the changes in cell surface chemical bonding and the composition of injured and repaired *S. aureus* cells. As depicted in Fig. 4 A, the signals primarily correspond to proteins, lipids, and functional groups such as hydroxyl, carboxyl, and amine present in polysaccharide molecules located in the cell membrane. Peaks were observed at 3279, 3116, 2562, 1641, 1139, 1178, 857, and 564 cm^{-1}. Characteristic absorption peaks within the 3340-3050 cmˆ-1 range are attributed to the C-H stretching vibrations of membrane fatty acids, while those in the 1800-1500 cmˆ-1 range are associated with the amide I and II bands of proteins and peptides. Peaks within the 1200- 760 cm^{-1} range resulted from C-O-C stretching vibrations in glycosidic bonds. Furthermore, the protein secondary structure of injured *S. aureus* cells was analyzed within the 1600- 1700 cm^{-1} range (amide I band), which is associated with the C = O stretching vibration of amino acid residues. Fig. S 1, obtained from bands within the 1600- 1700 cm^{-1} range fitted by second-order derivatives, was used to analyze the distribution of bacterial proteins secondary structure, including α-helix, parallel and antiparallel β-sheet, β-turn, and random coil. For intact cells from the CK group, the proportions were as follows: 20.84% α-helix, 30.78% parallel and 13.53% antiparallel β-sheet, 14.31% β-turn, and 20.54% random coil (Fig. 4 E). In contrast, after treatment with OH, significant changes were observed: α-helix decreased to 17.58%, parallel β-sheet increased to 37.82%, antiparallel β-sheet decreased to 11.73%, β-turn decreased to 12.48%, and random coil decreased to 20.39%.

3.5. Analysis of cell proteins during repair

As illustrated in Fig. S 2, the protein bands of the CK group were intact and clear, whereas OH-treated cells displayed reduced protein band expression, with slight improvements observed after repair in NB. Furthermore, the expression and synthesis of membrane proteins during OH treatment and subsequent repair were investigated. As presented in Fig. 5A, the protein bands of untreated cells were complete and clear,

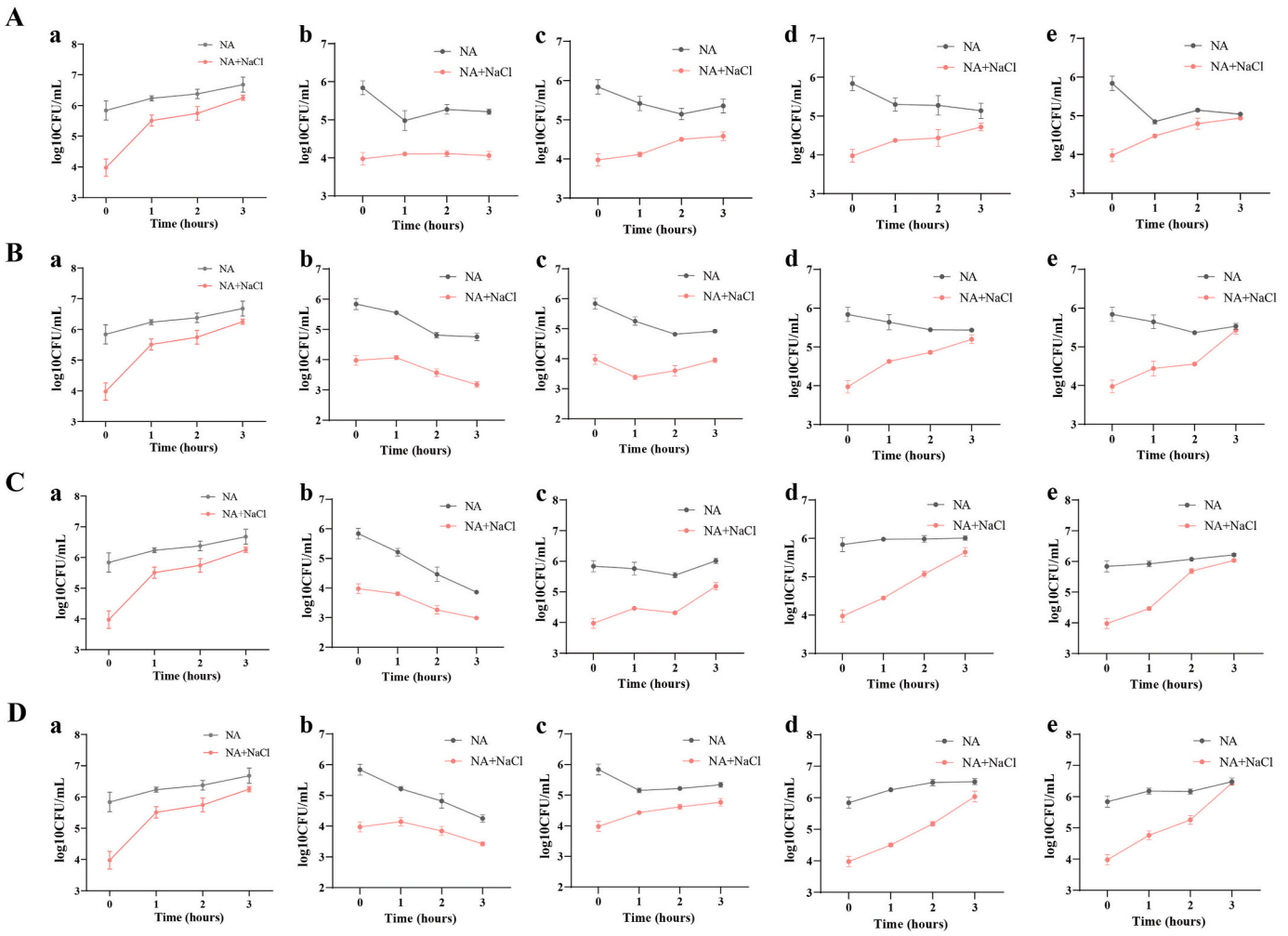

Fig. 6. Effects of different concentrations of chlorogenic acid (A), gallic acid (B), tea tree oil (C), carvacrol (D) on recovery of injured *S. aureus.* (A, B, C-a) NB, (A, B, C-b) NB with 0.625 mg/mL chlorogenic acid, gallic acid, tea tree oil; (A, B, C-c) NB with 0.313 mg/mL chlorogenic acid, gallic acid, tea tree oil; (A, B, C-d) NB with 0.156 mg/mL chlorogenic acid, gallic acid, tea tree oil; (A, B, C-e) NB with 0.078 mg/mL chlorogenic acid, gallic acid, tea tree oil; (D-a) NB, (D-b) NB with 0.078 mg/mL carvacrol, (D-c) NB with 0.039 mg/mL carvacrol, (D-d) NB with 0.020 mg/mL carvacrol, (D-e) NB with 0.010 mg/mL carvacrol. Error bars represent the standard deviations from three independent replicates.

while injured *S. aureus* cells exhibited a marked reduction in protein bands. Changes in band intensity and the disappearance of specific bands, particularly around 15 kDa, 25 kDa, and within the 50–70 kDa and 100–150 kDa ranges, suggest significant effects of OH treatment on membrane proteins. During restorations, some bands regained intensity, but others remained absent. Even after 5 h of repair, the injured *S. aureus* cells still differed from intact cells in both the number and intensity of protein bands.

3.6. Analysis of DNA during repair

Agarose gel electrophoresis was utilized to examine DNA changes in OH-induced sublethally injured and subsequently repaired *S. aureus* cells. As shown in Fig. 5 B, the molecular weight of the detected DNA fragments was consistently greater than 10,000 bp across all groups. Compared to the CK group, there was no noticeable change in the position of DNA bands in unrepaired injured *S. aureus* cells, the brightness of DNA bands significantly decreased and gradually increased during the repair process.

3.7. Effects of different bacteriostatic agents on the repair of injured S. aureus

The present study identified the detrimental effects of OH on *S. aureus* under mild conditions (55.5 °C) and highlighted the potential for self-repair in injured bacteria. Since severe OH treatment could compromise food products acceptability, investigating bacteriostatic agents to inhibit the viability of injured bacteria is crucial. Therefore, the effects of four common bacteriostatic agents—chlorogenic acid, gallic acid, tea tree oil, and carvacrol—on the repair process of injured *S. aureus* cells were analyzed using OH-induced injured *S. aureus* with a sublethal ratio >95% (initial cell counts of 5.84 and 3.98 $\log_{10}$ CFU/mL on NA and NA+ 10% NaCl, respectively). Taking chlorogenic acid as an example: Fig. 6A–a indicated that, in the absence of bacteriostatic agents, injured *S. aureus* cells repaired within 3 h, with no significant difference in cell counts between selective and non-selective media. Additionally, as the concentration of chlorogenic acid decreased, the bacteria's ability to repair gradually improved (Fig. 6 A–b, c, d, e). At concentrations of 0.156 and 0.078 mg/mL, after 3 h, although the count in NA did not increase significantly compared to 0 h, the injured *S. aureus* cells recovered significantly, and there was no difference in the count between the two media. Thus, the inhibition was concentration-dependent, with the lowest concentration of chlorogenic acid against

OH-induced injured *S. aureus* cells being 0.313 mg/mL. Gallic acid, tea tree oil and carvacrol exhibited similar trends, with the lowest effective concentrations identified as 0.156 mg/mL, 0.156 mg/mL, and 0.039 mg/mL, respectively. The inhibitory effects of EOs and PMs ranked as follows: carvacrol > chlorogenic acid and gallic acid > tea tree oil, respectively.

3.8. Effects of carvacrol on growth of sublethally injured S. aureus in pasteurized milk

As shown in Fig. S3, the viable counts on NA plates suggest that at 4 °C and 25 °C, the number of bacteria increased significantly during the first 0–6 h, while growth rates decreased dramatically after 6 h. The counting results from NA-NaCl plates indicated that OH-induced injured *S. aureus* could utilize nutrients from pasteurized milk for self-repair. At 4 °C, injured bacteria were still present in the milk at the end of the experiment, and the presence of carvacrol increased the proportion of injured *S. aureus* cells. When the storage temperature was 25 °C, the repair rate of injured bacteria was markedly accelerated, and there was no significant difference between NA and NA-NaCl plates by the end of the experiment.

Moreover, to explore the visual effects, samples with different treatments are shown in Fig. S4. Pasteurized milk is rich in proteins and lipids, serving as a high-quality medium for microorganisms to perform metabolic activities. After 72 h of storage at 4 °C, it was difficult to observe precipitate formation in all sample groups. However, storage at 25 °C caused the milk to coagulate and produce putrid gas. Thus, combining the results from Fig. S3, it was found that the combined effect of refrigeration with bacteriostatic agents inhibited precipitate formation in milk.

4. Discussion

Previously, the majority of research on the repair mechanisms of injured bacteria focuses on changes in the repair environment, while structural change is a relatively novel perspective (Lan et al., 2019; Lan & Shi, 2022; Shao et al., 2022). The present research first explored the alternations in bacteria biological characteristics (surface hydrophobicity, zeta potential, and particle size) during the repair period. The cell surface of bacteria contains various functional elements such as proteins and lipids, which significantly influence their structure, resistance and surface properties (Vimberg, Buriánková, Mazumdar, Branny, & Novotná, 2022). In the present research, OH treatment markedly reduced the values of biological characteristics, which were consistent with previous studies, spore particle size decreased significantly with reduced cell viability under intensified ultrasound or OH treatment conditions (Lv et al., 2019; Sun et al., 2024). A notable reduction in particle size may be also associated with damage to membrane proteins (Lv et al., 2019), and there was no significant difference compared to unrepaired injured cells after 5 h of repair, and it remained notably lower than that of the untreated group. This result suggests that OH treatment may disrupt cellular structure and cause damage to membrane proteins that are difficult to repair. In addition, damage to cell membrane structure led to a decrease in the absolute zeta potential (Shi, Li, Yang, Wei, & Huang, 2023), which was altered by OH treatment and did not return to normal level after 5 h of repair. Overall, these findings collectively indicate that the cellular structure of damaged *S. aureus* cells was not fully restored after 5 h of repair, highlighting the need for further analysis to understand the repair mechanisms.

Bacterial membrane potential, an electrochemical gradient formed by ionic differences across the cell membrane, is disrupted upon cell membrane damage. Our result indicated that OH treatment induced significant depolarization (Fig. 2 A), which was consistent with previous findings (Shao et al., 2023), and signifying that reduced selective permeability contributes partially to the formation of sublethally injured bacterial cells (Ning et al., 2022). Moreover, membrane depolarization and impaired membrane integrity often coincide with dysfunction of ion pumps and subsequent leakage of essential ions (Zhao, Shao, Jia, Meng, et al., 2022). During recovery in NB, the membrane potential and integrity gradually repaired, indicating a decrease in membrane damage (Fig. 2A and B). Similar to previous studies, no significant difference in bacterial counts was observed between non-selective and selective media after 2 h of repair in TSB. However, indicators related to cell membrane function, such as ion pump enzymes, had not fully recovered in the injured bacterial cells (Hao et al., 2022). Furthermore, the recovery of cell membrane potential is closely linked to ATP synthesis, reflecting cellular metabolic activity (Fang, Xu, Lin, Cai, & Wang, 2019), which may point to an increase proportion of cells capable of normal metabolic activities. Additionally, the increased intracellular ion content during repair is potentially linked to the restoration of membrane ion pumps and enhanced cell membrane integrity (Wang et al., 2024).

The cell wall, serving as a rigid protective barrier, maintains cell morphology, withstands osmotic pressure, and prevents the invasion of foreign substances (Wang et al., 2017; Zhao et al., 2021). Gram-positive bacteria, such as *S. aureus,* typically possess thicker cell walls. AKP, a protease located between the cell wall and the membrane, is commonly used to assess cell wall integrity. Additionally, AKP is involved in phosphate group transfer and metabolism in microbes, influencing various cellular processes such as protein production, DNA and RNA synthesis, lipid metabolism, and calcium ion regulation (Liao, Chen, Sant'Ana Anderson, Feng, & Ding, 2023). LDH plays a crucial role in several biological processes including biofilm formation, virulence maintenance, and resistance to external damage (Shu et al., 2022). Disruption of bacterial structural integrity results in decreased intracellular LDH content (Wang et al., 2017). Previous research has shown that damage to the cell structure leads to significant leakage of LDH and AKP, along with substantial leakage of protein and nucleic acid, which reduce the viable cell's resistance to essential oil and leading to gradual cell death (Bai et al., 2023).

In the present study, AKP and LDH activities decreased following OH treatment, suggesting damage to the cell membrane and walls. In contrast, enzyme levels gradually increased during the repair process, potentially due to the restoration of cellular structure and reactivation of metabolic pathways. Previous research has highlighted significant recovery of virulence-related indicators in sublethally injured *S. aureus* during repair (Shao et al., 2022), underscoring the critical role of LDH activity restoration. Therefore, the presence of sublethally injured bacteria and associated risks in OH-treated foods necessitate attention. Apart from thermal effects, OH likely induce non-thermal effects that continues to affect the cell wall by accumulating charges after cell membrane damage, thereby suppressing peptidoglycan synthesis. The peptidoglycan contents serve as a molecular indicator of cell wall integrity (Ning et al., 2022). Consistent with prior research, a decrease in peptidoglycan content typically signifies cell wall damage due to bacterial structural disruption (Shi et al., 2023). β-galactosidase is considered a key enzyme regulating cell wall synthesis and is often used to assess microbial structural integrity and the extent of bacterial disruption (Shu et al., 2022; Yang et al., 2023). In the present research, the alternating trends of peptidoglycan content and β-galactosidase during repair indicate a short-term activation of cell structure synthesis enzymes to expedite cell repair (Fig. 2E and F). Overall, in this study, cell membrane potential, membrane integrity, and cell wall-related indices revealed that OH treatment disrupts the cellular structure of *S. aureus* cells, which is gradually restored during repair. This phenomenon aligns with the hypothesis that recovery of the outer cellular structure is crucial for repairing sublethally injured bacteria cells (Rivas et al., 2013; Suo et al., 2018). Changes in microscopic morphology (SEM and TEM) supported the aforementioned variations in indicators (Fig. 3). Notably, the synchronization of membrane and cell wall recovery during the repair process was not observed, indicating the complexity of repairing OH-induced bacteria injuries from the perspective of cellular structure changes.

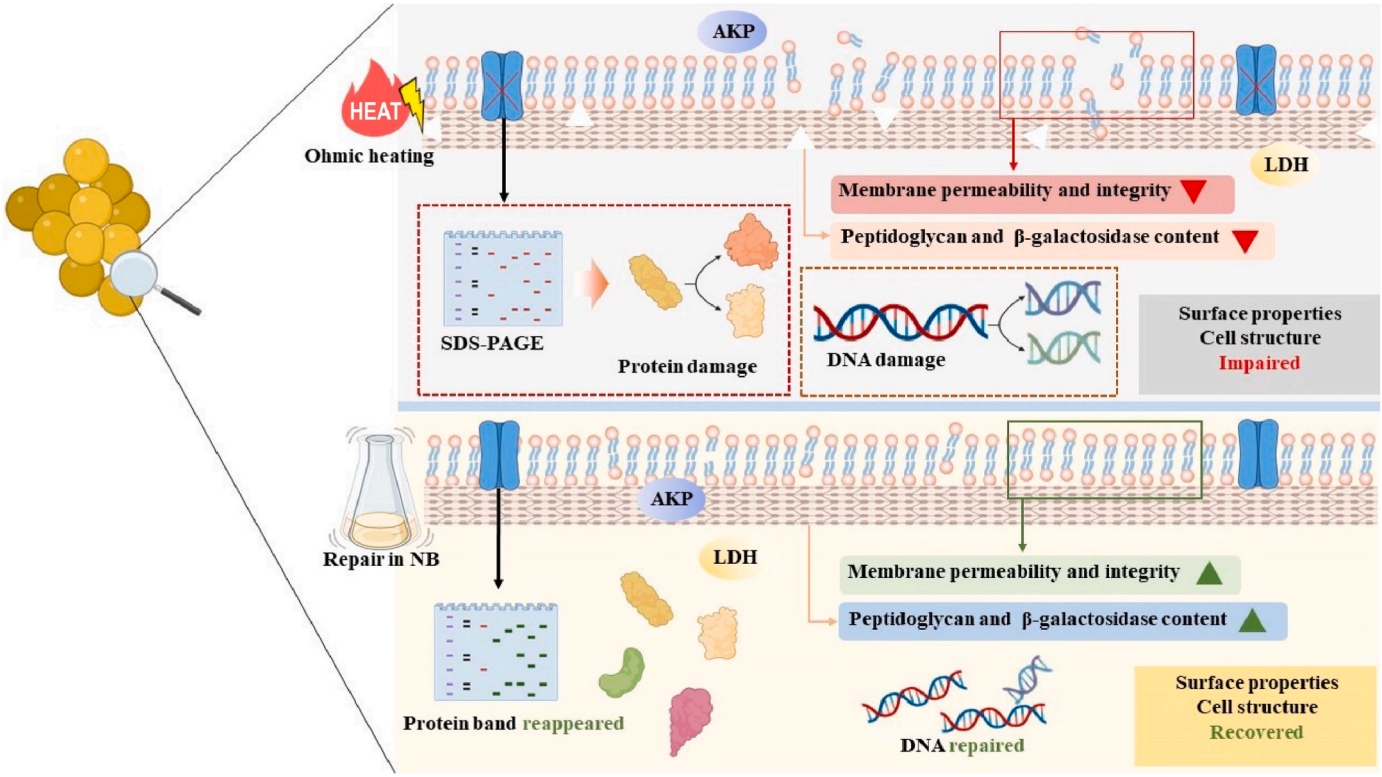

Fig. 7. Schematic diagram of the potential mechanisms of the formation and repair of sublethally injured *S. aureus* cells induced by OH treatment.

The results of FTIR analysis suggested that OH treatment damaged cell membrane, including alterations in membrane fatty acid, modifications in protein structure, and disruptions in carbohydrate backbones. Subsequent examinations uncovered that the secondary structure of *S. aureus* cell proteins was destroyed by OH, which may potentially affect hydrogen bonds (Nasiru et al., 2022; Qian et al., 2022). Similar to other indicators, slight alternations (Fig. 4) in some absorption signals indicate the restoration of the cell surface's chemical composition, while certain bacteria protein structures (Fig. S1) were challenging to repair.

Based on the above observations, OH treatment appears to disrupt the protein function of *S. aureus* cells. Previous studies have demonstrated that OH treatment led to a marked increase in protein leakage and inhibited the synthesis of proteins crucial for energy metabolism, osmotic pressure regulation, and cell membrane-associated functions (Shao et al., 2020; Tian et al., 2019). However, the molecular weight distribution of proteins in bacteria under different states remains unclear. In the present research, the results of SDS-PAGE suggested that proteins molecular weight distribution of proteins changed after OH treatment, with slight improvements observed after repair in NB. This indicates that sublethally injured bacteria might utilize nutrients to partially restore the damaged protein synthesis pathways. In addition, cell membrane proteins play pivotal roles in transportation, recognition, and maintenance of cell structure, which are critical for the normal physiological functioning of the cell membrane. The results of SDS-PAGE indicated that OH damaged the membrane of *S. aureus* cells, and the membrane proteins may not fully recover after repair (Fig. 5 A). These SDS-PAGE results were consistent with morphological observations (SEM and TEM) and cell membrane-related indices (membrane potential and integrity). Overall, it can be inferred that complete membrane repair is not a prerequisite for the reproductive capability of bacterial cells under suitable conditions.

The impairment of DNA structure is considered one of the significant mechanisms contributing to the bactericidal effects of novel technological techniques (Wang et al., 2023). In the present research, the observed changes in DNA band brightness can be attributed to both the thermal and non-thermal effects of OH treatment (Fig. 5 B). According to prior research, OH treatment disrupts DNA synthesis and affects the expression of proteins involved in DNA repair and transcription, leading to DNA damage and degradation (Shao et al., 2021). The gradual increase in band brightness during repair further supports the notion that sublethally injured *S. aureus* cells are capable of repairing DNA damage under conducive growth conditions. In summary, agarose gel electrophoresis analysis provides valuable insights into the DNA structural changes in OH-induced sublethally injured and repaired *S. aureus* cells, highlighting the cellular response to sublethal stress and the repair mechanisms employed by bacteria to maintain genomic integrity.

Recently, the co-processing of novel technologies with methods such as bacteriostatic agents have been recognized as a potential means of ensuring food safety while maximizing food quality retention (de Souza Pedrosa et al., 2021). The use of natural active substances extracted from plants as bacteriostatic agents not only inhibits the proliferation of food-borne pathogenic and spoilage bacteria but also enhance flavor (He, Zhang, Zeng, Wang, & Brennan, 2018). Recent studies have demonstrated that PMs (chlorogenic acid and gallic acid) and EOs (tea tree oil and carvacrol) effectively inhibit foodborne pathogens, including *S. aureus*, *Escherichia coli*, and *Listeria monocytogenes* by damaging cell morphology, disrupting cell membranes, inhibiting energy metabolism, and causing the destruction of intracellular macromolecules (Bai et al., 2019; Pajohi Alamoti et al., 2022; Pang et al., 2022; Upadhyay et al., 2017). Additionally, ROS production has been identified as a mechanism contributing to the suppression of bacterial repair process (Du, Zhou, Liu, Chen, & Li, 2018). However, the industrial application of bacteriostatic agents faces challenges, such as potential deterioration of food's organoleptic qualities due to excessive concentration, and volatilization during storage, which reduces their bacteriostatic effect (Cava-Roda, Taboada-Rodríguez, Valverde-Franco, & Marín-Iniesta, 2012). Therefore, inducing sublethal injury in bacteria through OH and then determining the minimum inhibitory concentration of bacteriostatic agents can facilitate the industrial application of this combined method. In this study, we identified the minimum

effective concentrations of four bacteriostatic agents needed to prevent the recovery of injured bacteria cells. Furthermore, the inhibitory effect of combined treatment with OH and carvacrol on contaminated milk was investigated (Fig. S 3 and S 4). Notably, the inhibitory effect of carvacrol on the repair process was significantly diminished in different repair media, which may be related to the high nutrient content of pasteurized milk (Wang et al., 2024). These insights not only enhance our understanding of the repair mechanisms of sublethally injured cells and propose novel approaches to inhibit such repair during food processing, but also suggests that future studies could explore synergistic effects with other antimicrobial strategies to optimize their efficacy in food preservation. Fig. 7 illustrates the potential mechanisms underlying the formation and repair of sublethally injured *S. aureus* cells, inferred from changes in cell structure-related indicators in this research. Overall, our findings further suggest that the challenging recovery of cellular biological properties, including membrane integrity, membrane proteins, and surface functional groups, may serve as critical markers of sublethally damaged bacteria. These insights underscore the complex nature of bacterial injury and repair processes, highlighting areas for future research and potential strategies for microbial control in various applications.

5. Conclusion

In conclusion, our data first demonstrated that the biological properties (impaired surface hydrophobicity, zeta potential, and particle size) and associated cell structures (the integrity of cell membrane and cell wall, and protein structure) of sublethally injured *S. aureus* were compromised by OH treatment and recovered to various degrees after repair in NB. Second, joint processing of OH treatment under mild parameters and bacteriostatic agents (chlorogenic acid, gallic acid, tea tree oil, and carvacrol) is a potential approach to guaranteeing food safety, and the inhibitory effects of bacteriostatic agents was: carvacrol > chlorogenic acid and gallic acid > tea tree oil. Finally, combined treatment with carvacrol low temperatures effectively inhibited the repair of injured *S. aureus* cells in pasteurized milk; and reduced coagulate, precipitate formation, and produce putrid gas in milk. This investigation not only demonstrates that the restoration of reproductive capacity in bacteria does not necessarily require a complete return to the untreated state, but also provides a theoretical basis for developing combined bacteriostatic methods aimed at enhancing food safety during storage.

CRediT authorship contribution statement

Han Wang: Writing – original draft, Methodology, Investigation, Data curation. **Lele Shao:** Methodology, Data curation. **Yingying Sun:** Methodology, Data curation. **Yana Liu:** Data curation. **Bo Zou:** Data curation. **Yijie Zhao:** Supervision, Data curation. **Yuhan Wang:** Supervision, Data curation. **Xingmin Li:** Writing – review & editing, Supervision, Conceptualization. **Ruitong Dai:** Writing – review & editing, Supervision, Methodology, Funding acquisition, Conceptualization.

Declaration of competing interest

The authors declare that they have no known competing financial interests or personal relationships that could have appeared to influence the work reported in this paper.

Acknowledgement

This work was supported by the National Natural Science Foundation of China (grant numbers 32272372).

Appendix A. Supplementary data

Supplementary data to this article can be found online at https://doi.org/10.1016/j.foodcont.2024.111086.

Data availability

The authors are unable or have chosen not to specify which data has been used.

References

Al-Shabib, N. A., Husain, F. M., Ahmad, I., Khan, M. S., Khan, R. A., & Khan, J. M. (2017). Rutin inhibits mono and multi-species biofilm formation by foodborne drug resistant Escherichia coli and Staphylococcus aureus. *Food Control*. https://doi.org/10.1016/j.foodcont.2017.03.004

Bai, J., Li, J., Chen, Z., Bai, X., Yang, Z., Wang, Z., et al. (2023). Antibacterial activity and mechanism of clove essential oil against foodborne pathogens. *Lebensmittel-Wissenschaft und -Technologie, 173*, Article 114249. https://doi.org/10.1016/j.lwt.2022.114249

Bai, H., Zhao, F., Li, M., Qin, L., Yu, H., Lu, L., et al. (2019). Citric acid can force Staphylococcus aureus into viable but nonculturable state and its characteristics. *International Journal of Food Microbiology, 305*, Article 10825. http://10.1016/j.ijfoodmicro.2019.108254.

Cava-Roda, R. M., Taboada-Rodríguez, A., Valverde-Franco, M. T., & Marín-Iniesta, F. (2012). Antimicrobial activity of vanillin and mixtures with cinnamon and clove essential oils in controlling Listeria monocytogenes and Escherichia coli O157:H7 in milk. *Food and Bioprocess Technology, 5*, 2120–2131. https://doi.org/10.1007/s11947-010-0484-4

de Souza Pedrosa, G. T., Pimentel, T. C., Gavahian, M., de Medeiros, L. L., Pagán, R., & Magnani, M. (2021). The combined effect of essential oils and emerging technologies on food safety and quality. *Lebensmittel-Wissenschaft und -Technologie, 147*, Article 111593. https://doi.org/10.1016/j.lwt.2021.111593

Du, W., Zhou, M., Liu, Z., Chen, Y., & Li, R. (2018). Inhibition effects of low concentrations of epigallocatechin gallate on the biofilm formation and hemolytic activity of Listeria monocytogenes. *Food Control, 85*, 119–126. https://doi.org/10.1016/j.foodcont.2017.09.011

Fang, Z., Xu, L., Lin, Y., Cai, X., & Wang, S. (2019). The preservative potential of Octopus scraps peptides−Zinc chelate against Staphylococcus aureus: Its fabrication, antibacterial activity and action mode. *Food Control, 98*, 24–33. https://doi.org/10.1016/j.foodcont.2018.11.015

Gavahian, M., & Farahnaky, A. (2018). Ohmic-assisted hydrodistillation technology: A review. *Trends in Food Science & Technology, 72*, 153–161. https://doi.org/10.1016/j.tifs.2017.12.014

Hao, J.-Y., Lei, Y.-Q., Shi, J.-Y., Zhao, W.-B., Gan, Z.-L., Hu, X., et al. (2022). Integrative physiological and transcriptome analysis reveals the mechanism for the repair of sub-lethally injured Escherichia coli O157: H7 induced by high hydrostatic pressure. *Foods, 11*, 2377. https://doi.org/10.3390/foods11152377

He, T.-F., Zhang, Z.-H., Zeng, X.-A., Wang, L.-H., & Brennan, C. S. (2018). Determination of membrane disruption and genomic DNA binding of cinnamaldehyde to Escherichia coli by use of microbiological and spectroscopic techniques. *Journal of Photochemistry and Photobiology B: Biology, 178*, 623–630. https://doi.org/10.1016/j.jphotobiol.2017.11.015

Huang, Z., Jia, S., Zhang, L., Liu, X., & Luo, Y. (2019). Inhibitory effects and membrane damage caused to fish spoilage bacteria by cinnamon bark (Cinnamomum tamala) oil. *Lebensmittel-Wissenschaft und -Technologie, 112*, Article 108195. https://doi.org/10.1016/j.lwt.2019.05.093

Huang, Z., Liu, X., Jia, S., Zhang, L., & Luo, Y. (2017). The effect of essential oils on microbial composition and quality of grass carp (Ctenopharyngodon idellus) fillets during chilled storage. *International Journal of Food Microbiology*. https://doi.org/10.1016/j.ijfoodmicro.2017.11.003

Ikuta, K. S., Swetschinski, L. R., Robles Aguilar, G., Sharara, F., Mestrovic, T., Gray, A. P., et al. (2022). Global mortality associated with 33 bacterial pathogens in 2019: A systematic analysis for the global burden of disease study 2019. *The Lancet, 400*, 2221–2248. https://doi.org/10.1016/S0140-6736(22)02185-7

Kobayashi, S. D., Malachowa, N., & DeLeo, F. R. (2015). Pathogenesis of Staphylococcus aureus abscesses. *American Journal Of Pathology, 185*, 1518–1527. https://doi.org/10.1016/j.ajpath.2014.11.030

Lan, L., & Shi, H. (2022). New insights into the formation and recovery of sublethally injured Escherichia coli O157: H7 induced by lactic acid. *Food Microbiology, 102*, Article 103918. https://doi.org/10.1016/j.fm.2021.103918

Lan, L., Zhang, R., Zhang, X., & Shi, H. (2019). Sublethal injury and recovery of Listeria monocytogenes and Escherichia coli O157: H7 after exposure to slightly acidic electrolyzed water. *Food Control, 106*, Article 106746. https://doi.org/10.1016/j.foodcont.2019.106746

Li, X., Zhang, J., Zhang, H., Shi, X., Wang, J., Li, K., et al. (2022). Genomic analysis, antibiotic resistance, and virulence of Staphylococcus aureus from food and food outbreaks: A potential public concern. *International Journal of Food Microbiology, 377*, Article 109825. https://doi.org/10.1016/j.ijfoodmicro.2022.109825

Liao, X., Chen, X., Sant'Ana Anderson, S., Feng, J., & Ding, T. (2023). Pre-Exposure of foodborne Staphylococcus aureus isolates to organic acids induces cross-adaptation to mild heat. *Microbiology Spectrum, 11*, Article e03832. https://doi.org/10.1128/spectrum.03832-22, 22.

Lv, R., Zou, M., Chen, W., Zhou, J., Ding, T., Ye, X., et al. (2019). Ultrasound: Enhance the detachment of exosporium and decrease the hydrophobicity of Bacillus cereus

spores. *Lebensmittel-Wissenschaft und -Technologie, 116*, Article 108473. https://doi.org/10.1016/j.lwt.2019.108473

Makroo, H. A., Rastogi, N. K., & Srivastava, B. (2020). Ohmic heating assisted inactivation of enzymes and microorganisms in foods: A review. *Trends in Food Science & Technology, 97*, 451–465. https://doi.org/10.1016/j.tifs.2020.01.015

Nasiru, M. M., Boateng, E. F., Wang, Z., Yan, W., Zhuang, H., & Zhang, J. (2022). Ultrasound-Assisted high-voltage cold atmospheric plasma treatment on the inactivation and structure of lysozyme: Effect of treatment voltage. *Food and Bioprocess Technology, 15*, 1866–1880. https://doi.org/10.1007/s11947-022-02842-z

Ning, Y., Hou, L., Ma, M., Li, M., Zhao, Z., Zhang, D., et al. (2022). Synergistic antibacterial mechanism of sucrose laurate combined with nisin against Staphylococcus aureus and its application in milk beverage. *Lebensmittel-Wissenschaft und -Technologie, 158*, Article 113145. https://doi.org/10.1016/j.lwt.2022.113145

Noma, S., Kiyohara, K., Hirokado, R., Yamashita, N., Migita, Y., Tanaka, M., et al. (2017). Increase in hydrophobicity of Bacillus subtilis spores by heat, hydrostatic pressure, and pressurized carbon dioxide treatments. *Journal of Bioscience and Bioengineering*. https://doi.org/10.1016/j.jbiosc.2017.09.012

Ortuzar, J., Martinez, B., Bianchini, A., Stratton, J., Rupnow, J., & Wang, B. (2018). Quantifying changes in spore-forming bacteria contamination along the milk production chain from farm to packaged pasteurized milk using systematic review and meta-analysis. *Food Control*. https://doi.org/10.1016/j.foodcont.2017.11.038

Pajohi Alamoti, M., Bazargani-Gilani, B., Mahmoudi, R., Reale, A., Pakbin, B., Di Renzo, T., et al. (2022). Essential oils from indigenous Iranian plants: A natural weapon vs. Multidrug-resistant Escherichia coli. *Microorganisms*.

Pang, Y., Wu, R., Cui, T., Zhang, Z., Dong, L., Chen, F., et al. (2022). Proteomic response of Bacillus subtilis spores under high pressure combined with moderate temperature and random peptide mixture LK treatment. *Foods*.

Pedreira, A., Martínez-López, N., Vázquez, J. A., & García, M. R. (2023). Modelling the antimicrobial effect of food preservatives in bacteria: Application to Escherichia coli and Bacillus cereus inhibition with carvacrol. *Journal of Food Engineering*. https://doi.org/10.1016/j.jfoodeng.2023.111734

Qian, J., Ma, L., Yan, W., Zhuang, H., Huang, M., Zhang, J., et al. (2022). Inactivation kinetics and cell envelope damages of foodborne pathogens Listeria monocytogenes and Salmonella Enteritidis treated with cold plasma. *Food Microbiology, 101*, Article 103891. https://doi.org/10.1016/j.fm.2021.103891

Qu, Q., Cui, W., Huang, X., Zhu, Z., Dong, Y., Yuan, Z., et al. (2023). Gallic acid restores the sulfonamide sensitivity of multidrug-resistant Streptococcus suis via polypharmaceology mechanism. *Journal of Agricultural and Food Chemistry*. https://doi.org/10.1021/acs.jafc.2c06991

Rivas, A., Pina-Pérez, M. C., Rodriguez-Vargas, S., Zuñiga, M., Martinez, A., & Rodrigo, D. (2013). Sublethally damaged cells of Escherichia coli by Pulsed Electric Fields: The chance of transformation and proteomic assays. *Food Research International, 54*, 1120–1127. https://doi.org/10.1016/j.foodres.2013.01.014

Sakr, M., & Liu, S. (2014). A comprehensive review on applications of ohmic heating (OH). *Renewable and Sustainable Energy Reviews, 39*, 262–269. https://doi.org/10.1016/j.rser.2014.07.061

Santana-Gálvez, J., Cisneros-Zevallos, L., & Jacobo-Velázquez, D. A. (2017). Chlorogenic acid: Recent advances on its dual role as a food additive and a nutraceutical against metabolic syndrome. *Molecules*. https://doi.org/10.3390/molecules22030358

Shao, L., Liu, Y., Tian, X., Wang, H., Yu, Q., Li, X., et al. (2020). Inactivation of Staphylococcus aureus in phosphate buffered saline and physiological saline using ohmic heating with different voltage gradient and frequency. *Journal of Food Engineering, 274*, Article 109834. https://doi.org/10.1016/j.jfoodeng.2019.109834

Shao, L., Zhao, Y., Zou, B., Li, X., & Dai, R. (2022). Recovery and virulence factors of sublethally injured Staphylococcus aureus after ohmic heating. *Food Microbiology, 102*, Article 103899. https://doi.org/10.1016/j.fm.2021.103899

Shao, L., Zou, B., Zhao, Y., Sun, Y., Li, X., & Dai, R. (2023). Inactivation effect and action mode of ohmic heating on Staphylococcus aureus in phosphate-buffered saline. *Journal of Food Safety, 43*, Article e13052. https://doi.org/10.1111/jfs.13052

Shi, Y., Li, Y., Yang, K., Wei, G., & Huang, A. (2023). A novel milk-derived peptide effectively inhibits Staphylococcus aureus: Interferes with cell wall synthesis, peptidoglycan biosynthesis disruption reaction mechanism, and its application in real milk system. *Food Control, 144*, Article 109374. https://doi.org/10.1016/j.foodcont.2022.109374

Shu, G., Xu, D., Zhang, W., Zhao, X., Li, H., Xu, F., et al. (2022). Preparation of shikonin liposome and evaluation of its in vitro antibacterial and in vivo infected wound healing activity. *Phytomedicine, 99*, Article 154035. https://doi.org/10.1016/j.phymed.2022.154035

Sun, Y., Shao, L., Liu, Y., Zou, B., Wang, H., Li, X., et al. (2024). Inactivation of Bacillus cereus spores by ohmic heating: Efficiency and changes of spore biological properties. *International Journal of Food Microbiology*, Article 110784.

Suo, B., Yang, H., Wang, Y., Lv, H., Li, Z., Xu, C., et al. (2018). Comparative proteomic and morphological change analyses of Staphylococcus aureus during resuscitation from prolonged freezing. *Frontiers in Microbiology, 9*, 866. https://doi.org/10.3389/fmicb.2018.00866

Tian, X., Shao, L., Yu, Q., Liu, Y., Li, X., & Dai, R. (2019). Evaluation of structural changes and intracellular substance leakage of Escherichia coli O157:H7 induced by ohmic heating. *Journal of Applied Microbiology, 127*, 1430–1441. https://doi.org/10.1111/jam.14411

Tian, X., Yu, Q., Shao, L., Li, X., & Dai, R. (2018). Sublethal injury and recovery of Escherichia coli O157: H7 after ohmic heating. *Food Control, 94*, 85–92. https://doi.org/10.1016/j.foodcont.2018.06.028

Tingting, L. I. U., Cui, C., Song, Z., Guo, Y., Changqing, L. I. U., Lizi, X. U., et al. (2022). Attribution analysis of foodborne disease outbreaks caused by Staphylococcus aureus and its enterotoxin in China's Mainland from 2010 to 2020. *Chinese Journal of Food Hygiene, 34*, 1029–1034. https://doi.org/10.13590/j.cjfh.2022.05.026

Tong Steven, Y. C., Davis Joshua, S., Eichenberger, E., Holland Thomas, L., & Fowler Vance, G. (2015). Staphylococcus aureus infections: Epidemiology, pathophysiology, clinical manifestations, and management. *Clinical Microbiology Reviews, 28*, 603–661. https://doi.org/10.1128/cmr.00134-14

Tongnuanchan, P., & Benjakul, S. (2014). Essential oils: Extraction, bioactivities, and their uses for food preservation. *Journal of Food Science*. https://doi.org/10.1111/1750-3841.12492

Upadhyay, A., Arsi, K., Wagle, B. R., Upadhyaya, I., Shrestha, S., Donoghue, A. M., et al. (2017). Trans-cinnamaldehyde, carvacrol, and eugenol reduce Campylobacter jejuni colonization factors and expression of virulence genes in vitro. *Frontiers in Microbiology, 8*, 713. https://doi.org/10.3389/fmicb.2017.00713

Vimberg, V., Buriánková, K., Mazumdar, A., Branny, P., & Novotná, G. B. (2022). Role of membrane proteins in bacterial resistance to antimicrobial peptides. *Medicinal Research Reviews, 42*, 1023–1036. https://doi.org/10.1002/med.21869

Wang, Y., Liu, Y., Zhao, Y., Sun, Y., Duan, M., Wang, H., et al. (2023). Bactericidal efficacy difference between air and nitrogen cold atmospheric plasma on Bacillus cereus: Inactivation mechanism of Gram-positive bacteria at the cellular and molecular level. *Food Research International, 173*, Article 113204. https://doi.org/10.1016/j.foodres.2023.113204

Wang, H., Shao, L., Liu, Y., Sun, Y., Zou, B., Zhao, Y., et al. (2024). Changes in stresses sensitivity of ohmic heating-induced sublethally injured Staphylococcus aureus during repair: Potential mechanisms at the cellular and molecular levels. *International Journal of Food Microbiology, 422*, Article 110814. https://doi.org/10.1016/j.ijfoodmicro.2024.110814

Wang, F., Wei, F., Song, C., Jiang, B., Tian, S., Yi, J., et al. (2017). Dodartia orientalis L. essential oil exerts antibacterial activity by mechanisms of disrupting cell structure and resisting biofilm. *Industrial Crops and Products, 109*, 358–366. https://doi.org/10.1016/j.indcrop.2017.08.058

Wang, Z., Zhu, J., Li, W., Li, R., Wang, X., Qiao, H., et al. (2020). Antibacterial mechanism of the polysaccharide produced by Chaetomium globosum CGMCC 6882 against Staphylococcus aureus. *International Journal of Biological Macromolecules, 159*, 231–235. https://doi.org/10.1016/j.ijbiomac.2020.04.269

Wei, S., Tian, Q., Husien, H. M., Tao, Y., Liu, X., Liu, M., et al. (2023). The synergy of tea tree oil nano-emulsion and antibiotics against multidrug-resistant bacteria. *Journal of Applied Microbiology*. https://doi.org/10.1093/jambio/lxad131

WHO. (2024). Food safety. Retrieved from https://www.who.int/health-topics/food-safety.

Yang, Z., He, S., Wei, Y., Li, X., Shan, A., & Wang, J. (2023). Antimicrobial peptides in combination with citronellal efficiently kills multidrug resistance bacteria. *Phytomedicine, 120*, Article 155070. https://doi.org/10.1016/j.phymed.2023.155070

Yazgan, H., Ozogul, Y., & Kuley, E. (2019). Antimicrobial influence of nanoemulsified lemon essential oil and pure lemon essential oil on food-borne pathogens and fish spoilage bacteria. *International Journal of Food Microbiology*. https://doi.org/10.1016/j.ijfoodmicro.2019.108266

Zhang, R., Lan, L., & Shi, H. (2021a). Sublethal injury and recovery of Escherichia coli O157: H7 after freezing and thawing. *Food Control, 120*, Article 107488. https://doi.org/10.1016/j.foodcont.2020.107488

Zhang, R., Lan, L., & Shi, H. (2021b). Sublethal injury and recovery of Escherichia coli O157:H7 after freezing and thawing. *Food Control, 120*, Article 107488. https://doi.org/10.1016/j.foodcont.2020.107488

Zhao, M., Bai, J., Bu, X., Tang, Y., Han, W., Li, D., et al. (2021). Microwave-assisted aqueous two-phase extraction of phenolic compounds from Ribes nigrum L. and its antibacterial effect on foodborne pathogens. *Food Control*. https://doi.org/10.1016/j.foodcont.2020.107449

Zhao, Y., Shao, L., Jia, L., Meng, Z., Liu, Y., Wang, Y., et al. (2022). Subcellular inactivation mechanisms of Pseudomonas aeruginosa treated by cold atmospheric plasma and application on chicken breasts. *Food Research International, 160*, Article 111720. https://doi.org/10.1016/j.foodres.2022.111720

Zhao, Y., Shao, L., Jia, L., Zou, B., Dai, R., Li, X., et al. (2022). Inactivation effects, kinetics and mechanisms of air- and nitrogen-based cold atmospheric plasma on Pseudomonas aeruginosa. *Innovative Food Science & Emerging Technologies, 79*, Article 103051. https://doi.org/10.1016/j.ifset.2022.103051

Zhen, D., Zhang, S., Yang, A., Ma, Q., Deng, Z., Fang, J., et al. (2024). A supersensitive electrochemical sensor based on RCA amplification-assisted "silver chain"-linked gold interdigital electrodes and CRISPR/Cas9 for the detection of Staphylococcus aureus in food. *Food Chemistry, 440*, Article 138197. https://doi.org/10.1016/j.foodchem.2023.138197